Journal of Electronics and Electrical Engineering
https://ojs.wiserpub.com/index.php/JEEE

UNIVERSAL WISER PUBLISHER

Research Article

Influence of Externally Elevated Package Temperature on the In-Circuit Performance of Selected Low-Power BJTs and Operational Amplifiers

Anthony Chibuike Ohajianya*, Odepeli Moses, Israel Chukwuemeka Ndukwe

Department of Physics, Federal University of Technology, Owerri, Nigeria
* Correspondence: anthony.ohajianya@futo.edu.ng

Received: 27 December 2025; **Revised:** 10 March 2026; **Accepted:** 16 March 2026; **Published:** 25 March 2026

Abstract: The electrical characteristics and reliability of semiconductor devices can be significantly affected by increased temperature. This study investigated the effect of temperature on the electrical characteristics of some selected bipolar junction transistors (BC546, BC548, BC549, and C8050) and operational amplifiers (µA741, LF353N, and LM358N) over a temperature range of 25°C to 200°C. The parameters investigated include base–emitter voltage, collector–emitter voltage, collector current, and current gain for the transistors, and closed-loop voltage gain for the operational amplifiers. The results show that the base-emitter voltage of the transistors decreased with increasing temperature. The temperature coefficient of the transistors was also found to range approximately from -1.1 mV/°C to -1.5 mV/°C. This is in reasonable agreement with theoretical and reported values for silicon BJTs. The variations in the transistors' collector current and current gain as a result of changes in temperature were found to be device dependent. This reflects the differences in the internal structure and biasing sensitivity of the transistors. For the operational amplifiers, the µA741 showed a noticeable decrease in closed-loop voltage gain at high temperatures, whereas the LF353N exhibited slight variation while the LM358N demonstrated excellent stability within the investigated temperature range. The findings of this research confirm that the performance of even low-power electronic components can be significantly affected by heat generated by other components. It is therefore pertinent for electronic circuit designers and developers to consider the effect of ambient temperature on low-power components, so as to include features to mitigate such adverse effects and ensure the durability of the electronic devices.

***Keywords*:** temperature, transistors, operational amplifiers, current gain, voltage gain

1. Introduction

The performance characteristics of Bipolar Junction Transistors (BJTs) and operational amplifiers (op-amps) can be significantly impacted by increased temperature. An increase in the temperature of a transistor can stimulate variations in some of the transistor's parameters like leakage current, on-resistance, switching speed, and current gain (β) [1]. In semiconductor devices, high temperatures usually induce an increase in the intrinsic carrier concentration. This further produces an increase in the leakage current and alters the minority carrier lifetime. In transistors, these temperature-induced changes result in the alteration of the current gain and other related parameters [2] while in operational amplifiers, the changes can manifest in the alteration of input offset voltages and bias currents [3].

Copyright ©2026 Anthony Chibuike Ohajianya, et al.
DOI: https://doi.org/10.37256/jeee.5120269493
This is an open-access article distributed under a CC BY license
(Creative Commons Attribution 4.0 International License)
https://creativecommons.org/licenses/by/4.0/

The lifespan and reliability of semiconductor devices can also be affected by increased temperatures [4]. Excessive heat can lead to thermal runaway, causing devices to fail prematurely [5–7]. It is therefore pertinent for Engineers to ensure that their electronic circuit designs have thermal management features that will help the devices to operate within their specified temperature ranges. Increased temperatures can also affect the accuracy and precision of sensor measurements. This makes it necessary for sensor circuits to be calibrated and compensated to mitigate or eliminate temperature effects [8]. Such temperature-effect mitigation efforts are especially necessary in automotive, aerospace, and medical devices, where precise measurements are critical for the functionality and safety of the systems.

Temperature compensation methods such as employing temperature sensors to monitor and compensate for variations in the operating conditions, can help extenuate the effects of temperature on the accuracy of sensors [9]. By incorporating these strategies into their designs, engineers can improve the overall performance and reliability of semiconductor devices in a wide range of applications.

1.1 *Bipolar Junction Transistors*

Bipolar Junction Transistors (BJTs) are semiconductor devices widely used as switches and amplifiers. They consist of either npn or pnp layers, with charge transport controlled by minority carriers in both emitter–base and base–collector junctions. A BJT usually has at least three terminals to link to an external circuit. Today, some transistors are packaged separately, but many more are found together in integrated circuits. A transistor can increase a signal because the controlled (output) power can be higher than the controlling (input) power. Some commonly used low-power PN-junction bipolar transistors are BC547, BC548, BC549, and C8050.

In the active region, a forward-biased emitter–base junction and a reverse-biased collector–base junction allow a base current I_B to control a larger collector current I_C, yielding a current gain defined as

$$\beta = \frac{I_C}{I_B} \tag{1}$$

The exponential relationship between collector current, I_C and base–emitter voltage V_{BE} can be expressed by

$$I_C = I_S exp(\frac{qV_{BE}}{kT}) \tag{2}$$

where I_S is the reverse saturation current, q is the electron charge, k is Boltzmann's constant, and T is absolute temperature. This dependence makes BJTs inherently sensitive to thermal variation. As temperature rises, increased intrinsic carrier concentration enhances I_S, which reduces V_{BE} approximately at a rate of -2 mV/°C for silicon devices and consequently increases I_C for a constant V_{BE} [2, 10].

Experimental studies confirm that both static and dynamic characteristics of BJTs vary with temperature. For example, measured data on NPN transistor 2SC2120 show that an increase in temperature from 25°C to 130°C results in a marked rise in collector current and current gain, accompanied by a reduction in threshold voltage [11]. Such changes influence bias point stability and can lead to thermal runaway in inadequately biased circuits.

Leakage currents, such as I_{CBO}, also increase exponentially with temperature, contributing to shifts in operating point and affecting low-signal performance. High temperature can also alter capacitances and carrier mobilities, influencing frequency response and transition frequency. The maximum ratings and electrical characteristics of BC546, BC548, BC549, and C8050 transistors as provided by the manufacturers are shown in Table 1.

Table 1. Maximum ratings and electrical characteristics of BC546, BC548, BC549, and C8050 transistors (Source [12])

Parameter	BC546	BC548	BC549	C8050
Collector-Base Voltage, V_{CBO} (V)	80	30	30	40
Collector-Emitter Voltage, V_{CEO} (V)	65	30	30	40
Emitter-Base Voltage, V_{EBO} (V)	6	5	5	6
Collector Current (DC), I_C (mA)	100	100	100	1500
Collector Power Dissipation, P_C (mW)	500	500	500	1000
Junction Temperature, T_j (°C)	150	150	150	150
Storage Temperature Range, T_{STG} (°C)	-65 to +150	-65 to +150	-65 to +150	-65 to +150
Collector Cut-off Current, I_{CBO} at V_{CB} = 30 V, I_E = 0 (μA)	15	15	15	100
DC Current Gain, h_{FE} at V_{CE} = 5 V, I_C = 2 mA	800	800	800	300

1.2 *Operational amplifiers*

Operational amplifiers (op-amps) are integrated circuits constructed mostly out of transistors and resistors. These integrated circuits multiply an input signal to a larger output. Karl D. Swartzel Jr. invented the first op-amp in 1967, and he originally conceived them to do mathematical operations in analog computers, thus the "operation" part of op-amps' name [13]. We now use op-amps in many other applications, and they form the basis of many modern analog electronic circuits. An operational amplifier is basically a three-terminal device that consists of two high-impedance input terminals and one output terminal. One of the inputs is called the inverting input, marked with a negative sign; the other input is called the non-inverting input, marked with a positive. Other pins of the IC are for powering and voltage offsetting. Some of the commonly used op-amp ICs include UA741, LF353N (Figure 1), and LM358N.

While an ideal op-amp is assumed to have infinite open-loop gain and zero offset, practical devices exhibit finite gain, non-zero input offset voltage, and bias currents, all of which are influenced by temperature variations [14]. In negative feedback configurations, the closed-loop gain of an op-amp is primarily determined by external components. For an inverting amplifier (Figure 1a) and a non-inverting amplifier (Figure 1b), the closed-loop voltage gain is given by equations (3) and (4), respectively.

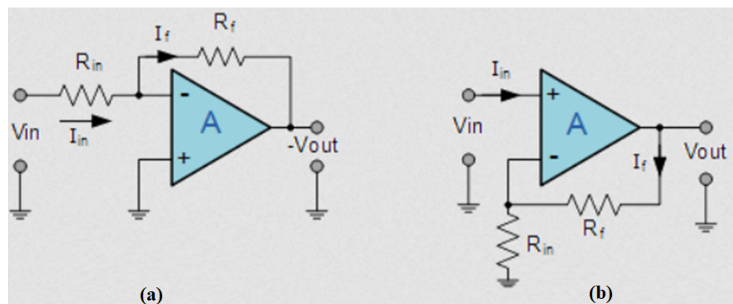

Figure 1. Operational amplifier configures as (a) inverting and (b) non-inverting amplifiers

$$A_{CL} = -\frac{R_f}{R_{in}} \quad \text{(for inverting amplifer)} \tag{3}$$

$$A_{CL} = 1 + \frac{R_f}{R_{in}} \quad \text{(for non-inverting amplifier)} \tag{4}$$

where R_f and R_{in} are the feedback and input resistances, respectively. Although feedback reduces sensitivity to internal parameter variations, temperature-dependent effects such as input offset voltage drift remain significant in precision applications.

The temperature dependence of the input offset voltage can be approximated by

$$V_{OS}(T) = V_{OS}(T_0) + (\frac{dV_{OS}}{dT})(T - T_0) \tag{5}$$

Where $V_{OS}(T)$ and $V_{OS}(T_0)$ are the input offset voltages at the operating temperature T (in kelvin or degrees Celsius) and reference temperature T_0 (typically 25°C), respectively, and $\frac{dV_{OS}}{dT}$ is the temperature coefficient of the offset voltage.

At elevated temperatures, increased leakage currents and reduced transconductance may lead to gain degradation and bandwidth reduction, affecting overall amplifier performance. A clear understanding of these temperature-induced variations is essential for reliable op-amp selection and circuit design, particularly in environments subject to wide temperature fluctuations.

Operational amplifiers are employed in many applications. Audio amplifiers, video processors, logic, memory, switches, radio frequency encoders and decoders are just a few examples. The maximum ratings and electrical characteristics of UA741, LM358N, and LF353N operational amplifiers as provided by the manufacturers are shown in Table 2.

Table 2. Maximum ratings and electrical characteristics of UA741, LM358N, and LF353N operational amplifiers (Source [12])

Parameter	UA741	LM358N	LF353N
Supply Voltage, V_{CC} (V)	±22	±16	±18
Input Voltage, V_I (V)	±15	±16	±15
Differential Input Voltage, V_{ID} (V)	±30	±32	±30
Power Dissipation, P_D (mW)	500	714	900
Operating Ambient Temperature Range, T_A (°C)	-55 to +125	0 to +70	0 to +70
Operating Junction Temperature, T_j (°C)	NA	150	115
Storage Temperature Range, T_{STG} (°C)	-65 to +150	-55 to +125	-65 to +150
Input Offset Voltage, V_{IO} at T_A = 25°C (mV)	5	7	10
Input Offset Current, I_{IO} at T_A = 25°C (nA)	20	50	4
Input Bias Current, I_{IB} at T_A = 25°C (nA)	100	-200	8
Large Signal Voltage Gain, A_V at V_O = ±10 V, R_L = 2 kΩ , T_A = 25°C	200	100	100

1.3 *Review of previous related works*

Research investigations on BJTs, mainly those fabricated with materials like 4H-SiC, have shown that high temperatures cause significant changes in the electrical characteristics. For instance, research findings have established that at increased temperatures, the specific on-resistance of 4H-SiC BJTs increases significantly from its lower values at room temperature [15, 16]. This is principally ascribed to the high-temperature-induced changes in mobility and recombination rates. In addition, the positive temperature coefficient observed in the on-resistance of some high-voltage BJTs helps in device paralleling, as shown in research where enhanced temperature stability was vital for reliable operation [17].

Temperature-induced changes can also influence the degradation mechanisms in BJTs. The degradation that thermal stress produces in semiconductor devices can be accelerated by high temperatures. This can manifest as shifts in threshold voltage, increase in leakage currents, and reductions in carrier mobility [18–21]. These perverse effects do not impact only the transistor's steady-state performance but also the dynamic parameters, including power dissipation and switching speeds. Electrothermal simulation tools are among the tools developed and used to forecast these temperature dependencies accurately so as to mitigate their effects [22].

The relationship between temperature and BJTs' performance is intricate. This is because the temperature-induced enhancement in some aspects of device operation may be followed by degradation in others. While BJTs fabricated with semiconductor materials like 4H-SiC show better thermal conductivity that helps reduce some high-temperature effects, in-depth evaluations reveal that even these devices display major performance shifts, such as increased on-resistance and reduced current gain, when subjected to protracted high-temperature conditions [16, 17, 23]. Consequently, cautious thermal management and robust electrothermal modeling are very important for the deployment of BJTs in high-temperature applications.

The performance of operational amplifiers (op-amps) is also affected by temperature variations. Some of the key parameters of op-amps, such as bandwidth, gain, offset voltage, bias currents, and noise performance, can be affected by high temperatures. As rising temperature usually causes semiconductor parameters, such as threshold voltage and carrier mobility, to vary, this in turn affects the behavior of the on-chip transistors and the overall circuit stability of op-amps. For instance, Baccar et al. evaluated the temperature-induced performance variations of op-amps [24]. They developed a behavioral model using VHDL-AMS that integrates temperature measurements to characterize these variations accurately. Their results highlight the significance of temperature effects on parameters like gain stability and offset voltage. Such models are important because they lay bare the dependency of op-amp performance on thermal conditions. They also provide a framework for forecasting the operational behavior of op-amps under varying temperatures.

Experimental investigations further corroborate these effects. In the study by Perov and Shevalye [25], the impact of heat treatment on op-amp performance was observed. From their results, they concluded that thermal stress could lead to notable degradations in op-amp parameters, which could be critical in precision applications. Complementing this, Yang et al. demonstrated that the use of chopper stabilization and careful circuit design can produce op-amps that maintain low input offset voltages and minimal drift across an extensive temperature range (from $-40°C$ up to $250°C$) [26]. Their work confirms that appropriate design techniques and compensation methods can mitigate the adverse effects of temperature changes, ensuring that the op-amp performance remains within acceptable limits for high-precision systems.

From a design viewpoint, the integration of robust design and Process-Voltage-Temperature (PVT) analysis is very important for achieving reliable op-amp operation in high-temperature conditions. Bendre and Kureshi reported that folded cascode op-amps showed desirable performance metrics over temperature ranges from $-40°C$ to $125°C$ [27]. This reveals that integrating temperature compensation into the design process helps in maintaining stability in the offset and gain of the op-amps. Such analyses, when combined with rigorous simulation methods, provide designers with predictive capabilities and allow for preemptive adjustments in manufacturing specifications. In this regard, the SPICE-based macromodel validation study conducted by Baccar et al. underscores the importance of simulation models that accurately reflect high-temperature performance, facilitating the prototyping and optimization of op amps without resorting to exhaustive thermal testing in the initial design phases [28].

In addition, ensuring operational stability under changing temperature conditions is not only important at the component level but also critical in the context of system-level applications. Terry et al. have demonstrated the development of robust analog electronics for extreme environments, such as those encountered in NASA/JPL projects, where operational amplifiers must perform reliably over a wide range of temperatures and continue to satisfy stringent performance criteria [29]. Their work demonstrates that incorporating thermal compensation methodologies and advancing macromodeling techniques into the design cycle is necessary for high-reliability applications, particularly in aerospace and automotive domains. Studies have also shown that temperature effects can be controlled through thoughtful design methodologies that include compensatory circuit techniques and robust testing protocols. [9, 30, 31]. This vast understanding of temperature effects on BJTs and op-amp performance has enabled the development of devices that are not only high-performing under standard conditions but also durable in extreme thermal environments. This has significantly improved the reliability and longevity of electronic systems used in a variety of industries.

While extensive literature exists on intrinsic junction temperature effects and electrothermal modeling of semiconductor devices, relatively fewer experimental studies focus on the influence of externally imposed package-level temperature under low internal power dissipation conditions. For instance, classical investigations by researchers such as Szekely, Janke, Zarębski, and Nowakowski established the fundamental electrothermal behavior of semiconductor devices and developed analytical and modeling approaches for describing junction temperature effects and self-heating phenomena [32].

These studies primarily focused on intrinsic device temperature behavior and electrothermal modeling under conditions where heat generation originates within the semiconductor junction due to power dissipation.

In practical electronic assemblies, however, semiconductor devices may also experience temperature changes caused by external heating from neighboring components, such as power transistors, voltage regulators, transformers, or high-power resistors. Under such conditions, low-power components, including small-signal BJTs and operational amplifiers, may operate with minimal internal power dissipation while still experiencing elevated package temperatures due to heat transfer from their surroundings. Such externally induced thermal exposure can alter device parameters and shift circuit operating points, potentially affecting bias stability, reference voltages, and amplifier performance.

Motivated by this practical scenario, the present study experimentally investigates the influence of externally elevated package surface temperature on the in-circuit electrical characteristics of several commonly used BJTs (BC546, BC548, BC549, and C8050) and operational amplifiers (µA741, LF353N, and LM358N). The devices were intentionally biased at low currents so that internal power dissipation, and therefore junction self-heating, remained negligible compared with externally imposed heating. The objective is therefore not to extract intrinsic junction temperature coefficients but to examine how externally induced ambient heating affects the electrical behavior of widely used low-power devices operating under practical circuit conditions. By providing a comparative experimental analysis of the thermal sensitivity of these devices, the work offers insights relevant to component selection and thermal layout considerations in electronic circuit design.

Contributions of this study

The main contributions of this work are:

i. Experimental investigation of the influence of externally elevated package temperature on the in-circuit electrical characteristics of low-power BJTs and operational amplifiers operating under minimal internal power dissipation.

ii. Comparative evaluation of the thermal sensitivity of several widely used discrete BJTs (BC546, BC548, BC549, C8050) and operational amplifiers (µA741, LF353N, LM358N) under identical bias and heating conditions.

iii. Quantification of temperature-induced variations in base–emitter voltage, collector current, current gain, and closed-loop amplifier gain when the dominant heat source is external ambient heating rather than junction self-heating.

iv. Practical insights for circuit designers regarding the susceptibility of low-power analog components to thermal disturbances caused by neighboring heat-generating devices.

2. Materials and methods

The materials, electronic components, and equipment used in this research include Electrical heater, Digital Multimeters, Breadboard and Vero board, Thermometer, Batteries, Jumper wires, Resistors, Transistors (BC546, BC548, BC549, and C8050), and Operational amplifier ICs (uA741, LM358N, and LF353N).

The experimental procedure began with the soldering of the jumper wires onto the 8-pin IC carrier's pins. The IC carrier would be used to connect and hold in place all the electronic components for the experiments. With this done, the experimental circuit was then configured as shown in Figure 2. The digital multimeters were used to measure the input and output voltages while the thermometer was used to read the body temperature of the semiconductor device as it was heated. The digital multimeters and the thermometer were arranged in a way that their screens could be videoed with a camera simultaneously.

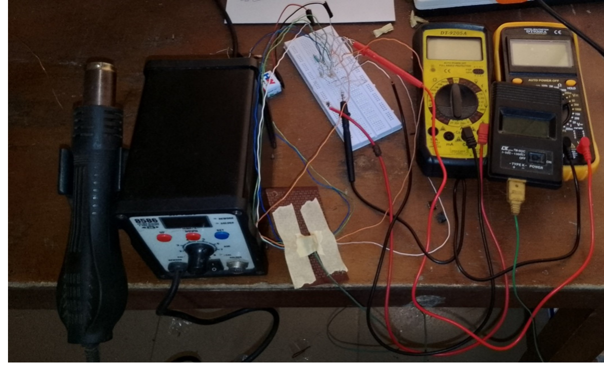

Figure 2. The experimental set up

2.1 *Transistor experiment*

The transistor experiment circuit was configured as shown in the circuit diagram of Figure 3. The thermometer's sensor wire was attached to the body of the first transistor (BC546) with a masking tape, and the transistor was plugged into the appropriate IC carrier ports. The circuit was powered-ON. The heater (which blows hot air) was then focused on the transistor, and the screens of the measuring meters were recorded with a camera as the body temperature of the transistor increased from 25°C to 200°C. From the video recordings, the readings of the transistor's base-emitter voltage (V_{BE}) and collector emitter voltage (V_{CE}) were extracted and recorded at intervals of 25°C. The reading screenshot for the BC546 transistor at 200°C ambient temperature is shown in Figure 4. The experiment was repeated with each of the remaining three transistors (BC548, BC549, and C8050) in place. The transistor's base current (I_b), collector current (I_c), and current gain (β) were calculated using equations (6), (7), and (8), respectively. The results were tabulated.

$$I_b = \frac{V_1 - V_{BE}}{R_1} \tag{6}$$

$$I_c = \frac{V_1 - V_{CE}}{R_2} \tag{7}$$

$$\beta = \frac{I_c}{I_b} \tag{8}$$

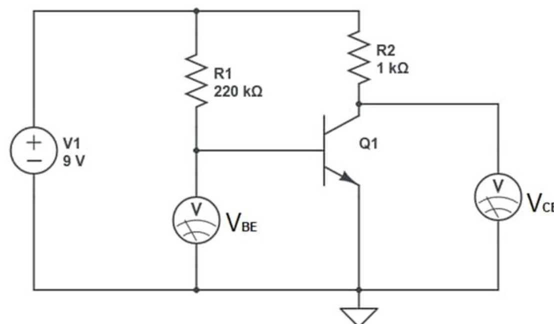

Figure 3. The transistor experiment circuit diagram

Figure 4. One of the reading screenshots for the BC546 transistor

2.2 *Operational amplifier (op-amp) IC experiment*

The op-amp IC circuit was configured as shown in Figure 5. The thermometer's sensor wire was attached to the top surface of the first op-amp IC (uA741) using a masking tape. The op-amp was then plugged into the IC carrier ports. The circuit was powered ON, and the heater was used to blow hot air on the op-amp IC. The screens of the measuring meters were recorded with a camera as the op-amp's body temperature increased from 25°C to 200°C. From the video recordings, the op-amp's input and output voltages were extracted and recorded at intervals of 25°C. The reading screenshot for the uA741 Op-Amp at 75°C body temperature is shown in Figure 6. The experiment was repeated with each of the remaining two Op-Amp ICs (LM358N and LF353N) in place. The closed-loop voltage gain of the op-amp was calculated using equation (9). The results were tabulated.

$$Voltage\ gain = \frac{V_{out}}{V_{in}} \tag{9}$$

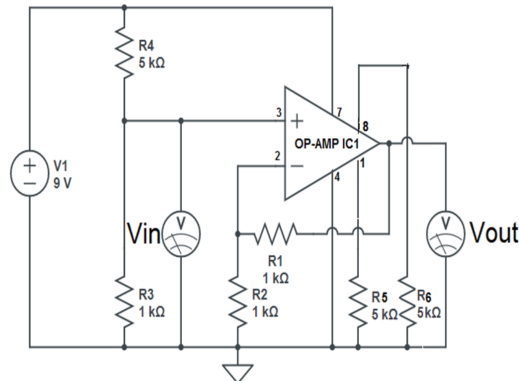

Figure 5. The op-amp experiment circuit diagram

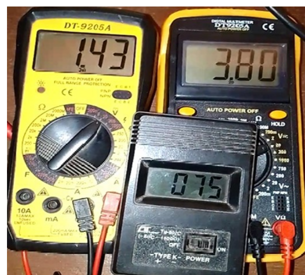

Figure 6. One of the reading screenshots for the uA741 op-amp

2.3 *External heating regime and low internal dissipation justification*

In this study, device heating was achieved through forced external convection using a hot-air blower directed at the package surface of the semiconductor device under test. The objective was to evaluate the influence of externally elevated package temperature on in-circuit electrical performance, rather than to investigate intrinsic junction self-heating effects.

All devices were biased under low-current operating conditions to ensure that internal power dissipation was minimal compared to the externally imposed thermal input. For the bipolar junction transistors, the collector current remained approximately in the range of 3–9 mA across the investigated temperature range. With collector–emitter voltages below 6 V in all cases, the maximum internal power dissipation was on the order of a few milliwatts. Such dissipation is negligible relative to the thermal energy supplied by forced hot-air convection. Consequently, junction temperature rise due to internal electrical power was minimal compared to externally imposed heating.

Because the dominant heat source in this experiment was external convection rather than internal dissipation, the measured package surface temperature is expected to be higher than the junction temperature during heating. Therefore, conventional junction self-heating relations of the form in equation (10) which apply when heat originates at the junction, are not directly applicable in this externally driven heating regime.

$$T_j = T_c + P_D \theta_{jc} \tag{10}$$

Where T_j = junction temperature, T_c = case temperature, P_d = power dissipation, and θ_{jc} = junction-to-case thermal resistance.

The present work thus evaluates device parameter variation as a function of externally elevated package temperature, simulating practical scenarios in which low-power components operate in proximity to heat-generating devices within electronic assemblies. The intent is to provide insight into thermal sensitivity under realistic ambient heating conditions rather than to extract intrinsic junction-temperature coefficients.

3. Results and discussion

The results of the transistor and operational amplifier experiments are hereby presented and discussed. Note that the results presented in this section reflect device parameter variations under externally imposed package temperature elevation while operating under low internal power dissipation. As discussed in Section 2.3, the dominant heat source in this study was forced external convection rather than junction self-heating. The measured temperature therefore represents the device package surface temperature under elevated ambient conditions. Consequently, the observed parameter variations correspond to in-circuit thermal sensitivity under externally induced thermal stress, simulating practical scenarios in which low-power components operate in proximity to heat-generating elements within electronic systems.

The discussion that follows interprets the results within this externally driven heating regime rather than as intrinsic junction-temperature characterization.

3.1 *Transistor test results*

Results of the transistor experiment are presented in Tables 3 and 4. From the results, bar charts of the transistors' base-emitter voltage against temperature and collector-emitter voltage against temperature were plotted as shown in Figures 7 and 8. Graphs of the collector current and current gain were plotted for the transistors as shown in Figures 9 to 12.

Table 3. Result of the transistor experiments for BC546 and BC548

Temp.		Transistor 1 (BC546)					Transistor 2 (BC548)				
S/N	(°C)	V_{BE} (V)	V_{CE} (V)	I_B (μ A)	I_C (mA)	β	V_{BE} (V)	V_{CE} (V)	I_B (μ A)	I_C (mA)	β
1	25	0.68	0.17	39.18	9.13	233	0.64	2.11	39.36	7.19	183
2	50	0.66	0.18	39.27	9.12	232	0.62	1.93	39.45	7.37	187
3	75	0.64	0.18	39.36	9.12	232	0.58	1.33	39.64	7.97	201
4	100	0.61	0.19	39.50	9.11	231	0.57	1.13	39.68	8.17	206
5	125	0.57	0.19	39.68	9.11	230	0.55	0.88	39.77	8.42	212
6	150	0.52	0.20	39.91	9.10	228	0.51	0.42	39.95	8.88	222
7	175	0.49	0.21	40.05	9.09	227	0.47	0.30	40.14	9.00	224
8	200	0.42	0.23	40.36	9.07	225	0.44	0.27	40.27	9.03	224

Table 4. Result of the transistor experiments for BC549 and C8050

Temp.		Transistor 3 (BC549)					Transistor 4 (C8050)				
S/N	(°C)	V_{BE} (V)	V_{CE} (V)	I_B (μ A)	I_C (mA)	β	V_{BE} (V)	V_{CE} (V)	I_B (μ A)	I_C (mA)	β
1	25	0.69	0.17	39.14	9.13	233	0.60	5.45	39.55	3.85	97
2	50	0.68	0.17	39.18	9.13	233	0.59	5.46	39.59	3.84	97
3	75	0.68	0.17	39.18	9.13	233	0.59	5.46	39.59	3.84	97
4	100	0.65	0.18	39.32	9.12	232	0.57	5.47	39.68	3.83	97
5	125	0.58	0.19	39.64	9.11	230	0.54	5.49	39.82	3.81	96
6	150	0.53	0.20	39.86	9.10	228	0.48	5.54	40.09	3.76	94
7	175	0.49	0.21	40.05	9.09	227	0.45	5.56	40.23	3.74	93
8	200	0.43	0.22	40.32	9.08	225	0.40	5.58	40.45	3.72	92

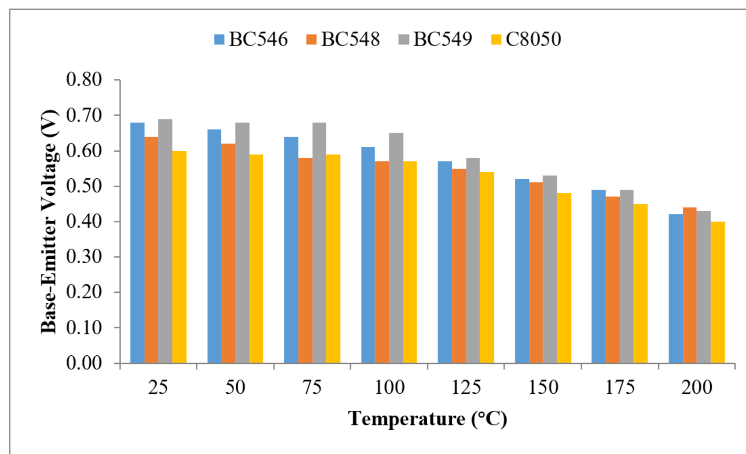

Figure 7. A bar chart of the transistors base-emitter voltage against temperature

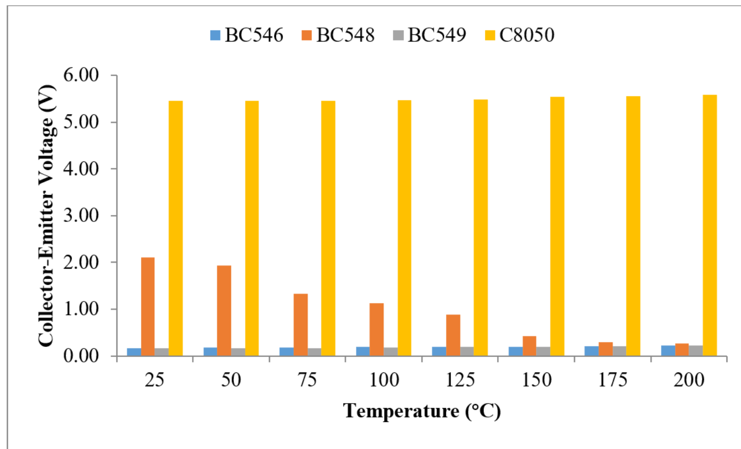

Figure 8. A bar chart of transistors' collector-emitter voltage against temperature

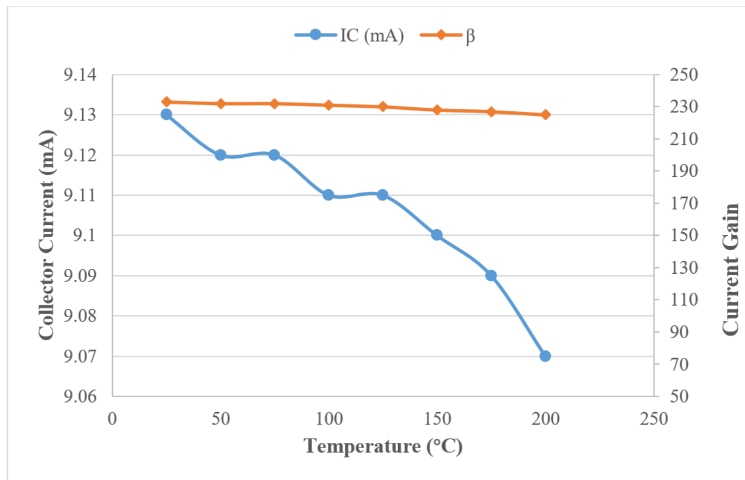

Figure 9. A graph of the BC546 collector current and current gain against temperature

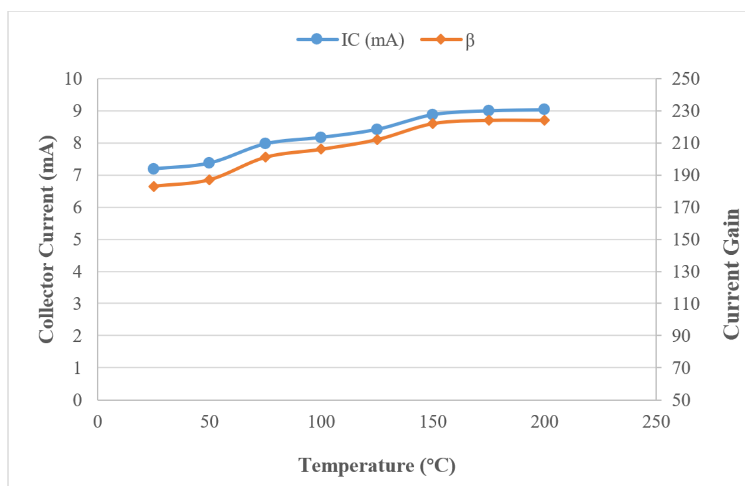

Figure 10. A graph of the BC548 collector current and current gain against temperature

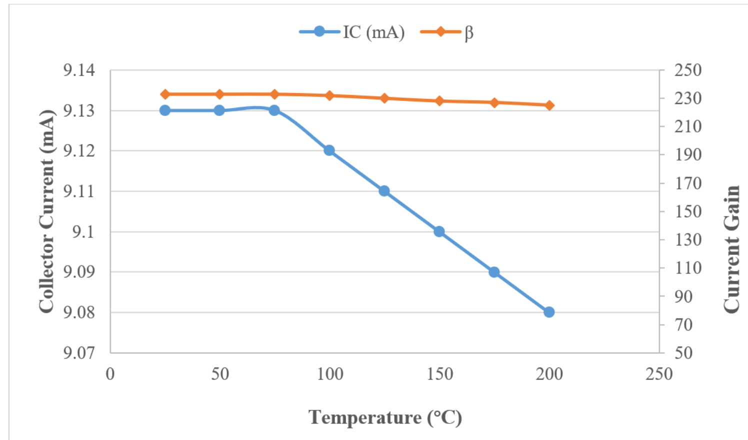

Figure 11. A graph of the BC549 collector current and current gain against temperature

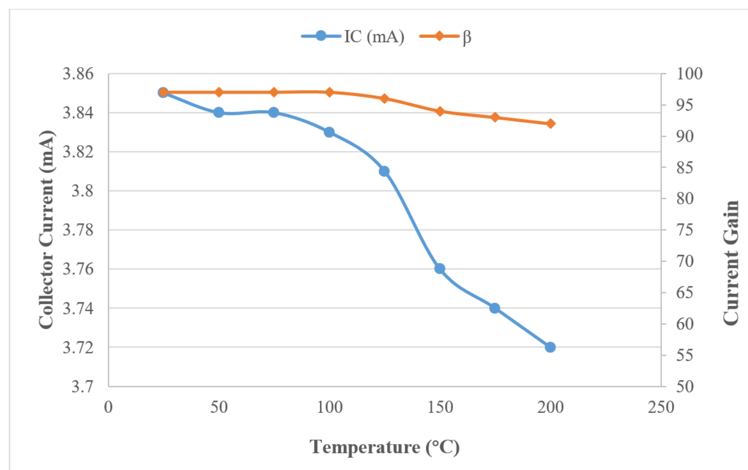

Figure 12. A graph of the C8050 collector current and current gain against temperature

The experimental results clearly demonstrate that device package temperature has a significant influence on the in-circuit electrical characteristics of the BJTs investigated (BC546, BC548, BC549, and C8050). One consistent trend observed across all the transistors is the decrease in base–emitter voltage (V_{BE}) with increasing temperature. This behavior is well established for silicon BJTs and is primarily attributed to the temperature dependence of the intrinsic carrier concentration and the saturation current, I_S, as described by the exponential collector current–base–emitter voltage relationship. As temperature increases, the saturation current increases exponentially, leading to a reduction in the required V_{BE} to sustain conduction. The observed reduction in V_{BE} is therefore consistent with the commonly reported temperature coefficient of approximately -2 mV/°C for silicon-based BJTs [33].

The collector–emitter voltage (V_{CE}) exhibited different trends among the transistors. For BC546, BC549, and C8050, V_{CE} increased slightly with temperature, whereas BC548 showed a decrease in V_{CE} with increasing temperature. These contrasting behaviors can be explained by differences in internal device structure, biasing conditions, and current gain variation with temperature. As temperature increases, changes in carrier mobility, leakage currents, and base recombination can shift the operating point of the transistor, even under fixed external biasing. In particular, the anomalous behavior observed in BC548 suggests that its temperature-dependent current gain increased sufficiently to alter the voltage distribution in the circuit, leading to a reduction in V_{CE}. Similar device-to-device variations have been reported in previous studies,

highlighting that transistors of the same family may respond differently to thermal stress due to manufacturing tolerances and internal doping profiles [34].

The collector current (I_C) and current gain (β) also showed temperature-dependent variations. For BC546 and BC549, both I_C and β exhibited a gradual reduction at higher temperatures, especially beyond 100 °C. This reduction can be attributed to increased recombination in the base region and reduced carrier mobility at elevated temperatures. In contrast, BC548 showed an increase in collector current and current gain with temperature, suggesting enhanced carrier injection efficiency within the studied temperature range. The C8050 transistor displayed relatively stable gain at lower temperatures, followed by a gradual decline at higher temperatures, which is consistent with thermal degradation effects reported for high-current BJTs [35].

Overall, these observations confirm that temperature-induced effects on BJTs are device-specific and depend not only on the transistor type but also on its internal construction and biasing conditions. It is important to emphasize that in the present configuration, the devices were biased with a fixed resistor network (Figure 3), and therefore parameter variations must be interpreted in the context of circuit-level operating point shifts. Since the base current is given by equation (6), a reduction in V_{BE} with increasing temperature leads to a slight increase in base current under fixed supply conditions. This effect is reflected in the experimental data, where I_B increases gradually with temperature (Tables 3 and 4). Consequently, changes in collector current and collector–emitter voltage arise from the combined effects of intrinsic semiconductor temperature dependence and bias network interaction.

The observed variations in V_{CE} among the devices can be directly understood from the circuit relationship of equation (7). Under this relation, any temperature-induced increase in collector current necessarily produces a decrease in V_{CE}, while a decrease in I_C results in an increase in V_{CE}. The differing V_{CE} trends among the transistors therefore reflect device-specific gain variations under externally elevated package temperature rather than anomalous behavior. This confirms that even under low-power bias conditions, externally imposed thermal stress can shift the operating point of small-signal BJTs in practical circuits.

These findings are particularly relevant for circuits where BJTs are used to establish reference voltages, bias currents, or sensor interfaces. Even when internal power dissipation is minimal, elevated ambient or neighboring component heat can alter V_{BE} and β sufficiently to affect precision performance.

3.2 *Operational amplifier test results*

Results of the operational amplifier experiments are presented in Table 5. From the results, a bar chart of the op-amps' closed-loop voltage gain against temperature was plotted as shown in Figure 13. Graphs of the op-amp closed-loop voltage gain against temperature for each op-amp were plotted as shown in Figures 14 to 16.

Table 5. Results of the op-amp experiment

Temp.		Op-Amp IC 1 (μA741)			Op-Amp IC 2 (LF353N)			Op-Amp IC 3 (LM358N)		
S/N	(°C)	V_{in} (V)	V_{out} (V)	Voltage Gain	V_{in} (V)	V_{out} (V)	Voltage Gain	V_{in} (V)	V_{out} (V)	Voltage Gain
1	25	1.43	3.89	2.72	1.40	2.67	1.91	1.41	2.84	2.01
2	50	1.43	3.83	2.68	1.40	2.67	1.91	1.41	2.84	2.01
3	75	1.43	3.80	2.66	1.40	2.67	1.91	1.41	2.84	2.01
4	100	1.43	3.76	2.63	1.40	2.72	1.94	1.41	2.84	2.01
5	125	1.43	3.66	2.56	1.40	2.73	1.95	1.41	2.84	2.01
6	150	1.43	3.40	2.38	1.40	2.74	1.96	1.41	2.84	2.01
7	175	1.43	3.16	2.21	1.40	2.78	1.99	1.41	2.84	2.01
8	200	1.43	2.88	2.01	1.40	2.82	2.01	1.41	2.83	2.01

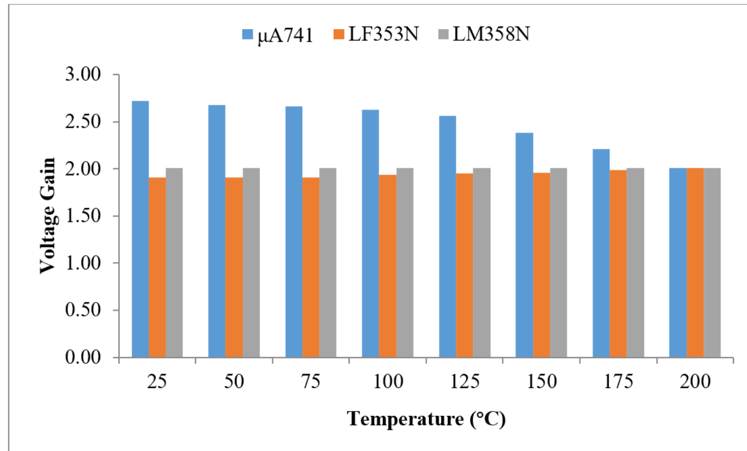

Figure 13. A bar chart of the operational amplifiers' voltage gain against temperature

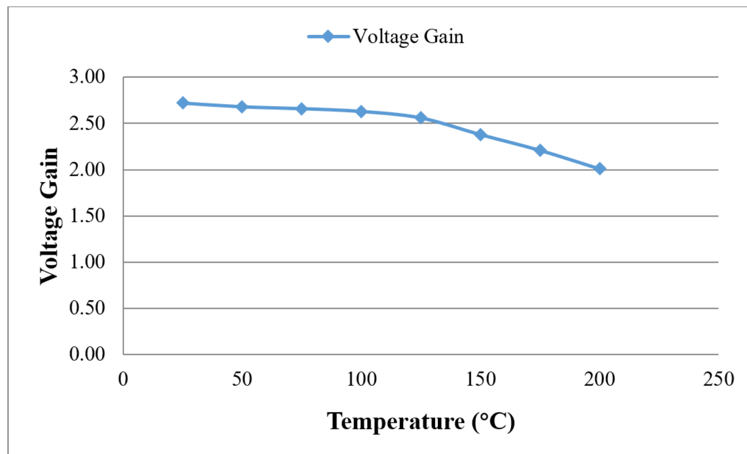

Figure 14. A graph of the uA741 op-amp voltage gain against temperature

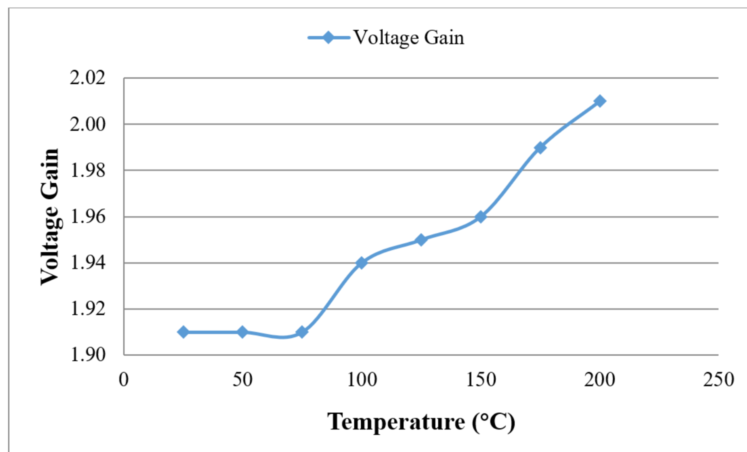

Figure 15. A graph of the LF353N op-amp voltage gain against temperature

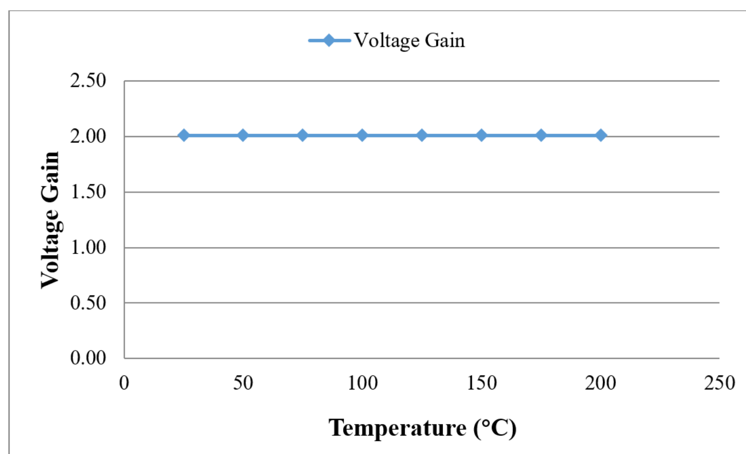

Figure 16. A graph of the LM358N op-amp voltage gain against temperature

The operational amplifier experiments focused on evaluating the in-circuit closed-loop voltage gain stability of µA741, LF353N, and LM358N under increasing device package temperature. The results indicate that temperature variations affected the op-amps differently, reflecting differences in their internal architecture and design objectives.

The µA741 operational amplifier showed a noticeable reduction in voltage gain as temperature increased from 25°C to 200°C. Although the closed-loop gain is primarily determined by external resistors, temperature-induced changes in internal parameters such as input offset voltage, bias currents, and transistor transconductance can influence the effective gain, especially at elevated temperatures. The µA741 is an older bipolar-input op-amp with limited thermal robustness, and its performance degradation at high temperatures aligns with the device manufacturer's data [12].

The LF353N operational amplifier exhibited relatively stable gain at lower temperatures, followed by a slight increase at higher temperatures. This behavior may be attributed to its JFET input stage, which generally offers improved thermal stability compared to bipolar input stages. The modest gain increase observed at higher temperatures could result from changes in internal bias currents and transconductance, which slightly alter the amplifier's internal operating conditions while still maintaining closed-loop stability.

In contrast, the LM358N operational amplifier demonstrated remarkable gain stability across the entire temperature range investigated. This stability highlights the robustness of the LM358 architecture, which is specifically designed for industrial and automotive applications where temperature variations are common. The observed stability supports its widespread use in environments requiring reliable analog performance under thermal stress.

It is important to emphasize that this study primarily evaluates closed-loop gain behavior. Due to the presence of negative feedback, temperature-induced variations in open-loop gain are largely suppressed. Consequently, parameters such as input offset voltage drift, input bias current variation, and output swing limitations, which are known to be strongly temperature-dependent, were not isolated in this experiment. Nevertheless, the results provide useful insight into the comparative thermal robustness of commonly used op-amps in practical circuit configurations.

3.3 *Quantitative temperature coefficients and comparison with literature*

To effectively compare the results of this work with literature, it pertinent to determine the temperature coefficient of the measured parameters.

3.3.1 *Base–emitter voltage temperature coefficient of BJTs*

From the experimental data, the temperature coefficient of the base–emitter voltage, V_{BE} for each transistor was estimated (as presented in Table 6) using the linear approximation over the temperature range of 25°C to 200°C (ΔT = 175°C) as given in equation (11).

$$\alpha V_{BE} = \frac{\Delta V_{BE}}{\Delta T} \tag{11}$$

Table 6. Temperature coefficient of the transistors' base-emitter voltage

Transistor	V_{BE} at 25°C (V)	V_{BE} at 200°C (V)	ΔV_{BE} (mV)	αV_{BE} (mV/°C)
BC546	0.68	0.42	−260	−1.49
BC548	0.64	0.44	−200	−1.14
BC549	0.69	0.43	−260	−1.49
C8050	0.60	0.40	−200	−1.14

The obtained temperature coefficients lie between -1.1 mV/°C and -1.5 mV/°C. This agrees with previous works as silicon BJTs have been consistently reported to have V_{BE} temperature coefficients of approximately -2 mV/°C near room temperature [2, 10, 11]. The slightly smaller magnitude observed in this work can be attributed to surface temperature measurement rather than true junction temperature, and non-uniform heating due to hot-air convection. Despite these limitations, the trend and order of magnitude agree well with theory and published experimental studies, confirming the validity of the measurements.

3.3.2 *Closed-loop gain temperature coefficient of operational amplifiers*

For the operational amplifiers, the closed-loop voltage gain temperature coefficient was estimated using equation (12) as presented in Table 7.

$$\alpha A_v = \frac{\Delta A_v}{\Delta T} \tag{12}$$

Table 7. Estimated temperature coefficient of the op-amps' closed-loop gain

Op-Amp	A_v at 25°C	A_v at 200°C	ΔA_v	αA_v (per °C)
µA741	2.72	2.01	−0.71	-4.1×10^{-3}
LF353N	1.91	2.01	+0.10	$+5.7\times 10^{-4}$
LM358N	2.01	2.01	0	0

The µA741 exhibited the largest negative gain temperature coefficient, indicating reduced internal transconductance and increased offset effects at elevated temperatures. This agrees with reports that bipolar-input op-amps such as the µA741 are thermally less robust compared to newer designs [24, 25].

The LM358N showed near-zero gain temperature coefficient, consistent with literature describing it as suitable for industrial and automotive environments where temperature stability is critical [27, 29].

The present results should therefore be interpreted as package-temperature-induced in-circuit parameter variations under externally driven heating conditions. Since internal power dissipation was intentionally kept low, the observed effects primarily reflect sensitivity to elevated ambient and neighboring-component heat rather than junction self-heating

phenomena. This distinction is important when comparing the present findings with studies focused on electrothermal modeling or intrinsic high-power device characterization.

4. Conclusion

This study has experimentally investigated the influence of externally elevated package surface temperature on the in-circuit electrical characteristics of selected low-power bipolar junction transistors (BC546, BC548, BC549, and C8050) and operational amplifiers (µA741, LF353N, and LM358N) operating under low internal power dissipation.

Unlike conventional electrothermal investigations focused on junction self-heating, the present work intentionally employed forced external convection to simulate realistic ambient-induced thermal stress conditions that may arise in electronic assemblies where low-power components operate in proximity to heat-generating devices. Because the devices were biased at low currents, internal power dissipation was minimal, and the observed parameter variations primarily reflect sensitivity to externally imposed package temperature.

For the BJTs, the base–emitter voltage consistently decreased with increasing surface temperature, with measured temperature coefficients ranging from approximately -1.1 mV/°C to -1.5 mV/°C over the investigated range. Although slightly lower in magnitude than the canonical -2 mV/°C often reported for intrinsic junction temperature behavior, these values confirm significant temperature sensitivity under externally elevated package conditions. The results further demonstrate device-dependent variations in collector current, current gain, and collector–emitter voltage arising from the interaction between intrinsic semiconductor temperature effects and fixed bias network constraints. These operating-point shifts highlight the susceptibility of bias and reference circuits to ambient thermal disturbances.

For the operational amplifiers, closed-loop gain stability was evaluated under identical heating conditions. The µA741 exhibited noticeable gain degradation at elevated surface temperatures, while the LF353N showed moderate variation. In contrast, the LM358N maintained nearly constant closed-loop gain across the investigated temperature range, indicating superior robustness under ambient thermal stress. These differences underscore the importance of architecture selection when designing circuits intended to operate in thermally dynamic environments.

Overall, the findings demonstrate that externally induced package temperature rise, even in the absence of significant internal self-heating, can produce measurable and architecture-dependent parameter drift in commonly used low-power discrete and integrated devices. The study therefore provides practical insight for circuit designers regarding component selection, thermal layout, and bias stability considerations in systems where localized heating may be present.

Future work may extend this approach by examining higher closed-loop gain configurations, isolating intrinsic offset and bias current drift, and incorporating controlled environmental chambers to further quantify ambient-induced thermal sensitivity.

Conflicts of interest

The authors declare that there is no conflict of interest regarding the publication of this paper.

References

[1] N. P. Allen, "Gallium nitride superjunction transistor (continued funding report)," 2022. https://doi.org/10.2172/1890078.

[2] R. Ibrahim, S. El-Azeem, S. El-Ghanam, and F. Soliman, "Temperature effects on the electrical characteristics of BJTs and MOSFETs," *Journal of Scientific Research in Science*, vol. 36, no. 1, pp. 100-112, 2019. https://doi.org/10.21608/jsrs.2019.30999.

[3] J. Huijsing, *Operational amplifiers*, Springer Cham, 2017. https://doi.org/10.1007/978-3-319-28127-8.

[4] M. Ohring and L. Kasprzak, *Reliability and Failure of Electronic Materials and Devices*, 2nd ed. London, U.K.: Academic Press, 2011. https://doi.org/10.1016/C2009-0-05748-1.

[5] O. Moses, A. C. Ohajianya, and I. C. Ndukwe, "Influence of temperature changes on the performance characteristics of some selected semiconductor PN-junction diodes," *Journal of Electronics and Electrical Engineering*, vol. 4, no. 2, pp. 67-82, 2025. https://doi.org/10.37256/jeee.4220257037.

[6] F. Iannuzzo, C. Abbate, and G. Busatto, "Instabilities in silicon power devices: a review of failure mechanisms in modern power devices," *IEEE Industrial Electronics Magazine*, vol. 8, no. 3, pp. 28-39, 2014. https://doi.org/10.1109/MIE.2014.2305758.

[7] J. C. Whitaker, "Semiconductor failure modes," in *Electronic Systems Maintenance Handbook*, 2nd ed. Boca Raton, FL, USA: CRC Press, 2001.

[8] A. J. Fleming, "A review of nanometer resolution position sensors: operation and performance," *Sensors and Actuators A: Physical*, vol. 190, pp. 106-126, 2013. https://doi.org/10.1016/j.sna.2012.10.016.

[9] A. J. Croxford, J. Moll, P. D. Wilcox, and J. E. Michaels, "Efficient temperature compensation strategies for guided wave structural health monitoring," *Ultrasonics*, vol. 50, no. 4-5, pp. 517-528, 2010. https://doi.org/10.1016/j.ultras.2009.11.002.

[10] A. Gruhle, "The influence of emitter-base junction design on collector saturation current, ideality factor, Early voltage, and device switching speed of Si/SiGe HBT's," *IEEE Transactions on Electron Devices*, vol. 41, no. 2, pp. 198-203, 1994. https://doi.org/10.1109/16.277379.

[11] G. T. Hasan, A. H. Mutlaq, and M. H. Husain, "Investigation of temperature effects on the characteristics of bipolar junction transistor," *BIO Web of Conferences*, vol. 97, 2024. https://doi.org/10.1051/bioconf/20249700110.

[12] AllDataSheet, "Electronic components datasheet search engine," [Online]. Available: https://www.alldatasheet.com. [Accessed Dec. 25, 2025].

[13] H. H. M. Tromp, "On designing functional artifacts," 2011. [Online]. Available: http://philosophygarden.nl/philosophy%20of/technology/Functional%20Artifact%20Design%20v4c3e.pdf. [Accessed Dec. 25, 2025].

[14] M. M. Choudhury, "Low voltage low power op-amp structures," 2024. [Online]. Available: https://oulurepo.oulu.fi/handle/10024/51217. [Accessed Dec. 25, 2025].

[15] S. Krishnaswami, A. Agarwal, S.-H. Ryu, C. Capell, J. Richmond, J. Palmour, et al., "1000-V, 30-A 4H-SiC BJTs with high current gain," *IEEE Electron Device Letters*, vol. 26, no. 3, pp. 175-177, 2005. https://doi.org/10.1109/LED.2004.842731.

[16] I. Perez-Würfl, J. Torvik, and B. Van Zeghbroeck, "Analysis of power dissipation and high temperature operation in 4H-SiC bipolar junction transistors with 4.9 MW/cm2 power density handling ability," *Materials Science Forum*, vol. 457-460, pp. 1121-1124, 2004. https://doi.org/10.4028/www.scientific.net/msf.457-460.1121.

[17] S.-H. Ryu, A. K. Agarwal, R. Singh, and J. W. Palmour, "1800 V NPN bipolar junction transistors in 4H-SiC," *IEEE Electron Device Letters*, vol. 22, no. 3, pp. 124-126, 2001. https://doi.org/10.1109/55.910617.

[18] N. Toufik, F. Pélanchon, and P. Mialhe, "Degradation of junction parameters of an electrically stressed NPN bipolar transistor," *Active and Passive Electronic Components*, vol. 24, no. 3, pp. 155-163, 2001. https://doi.org/10.1155/2001/53209.

[19] J. Atterstig, "Establishing high-temperature models for leakage current in gated lateral bipolar junction transistors," 2024. [Online]. Available: https://www.diva-portal.org/smash/record.jsf?pid=diva2:1845006. [Accessed Dec. 25, 2025].

[20] S. Jahdi, M. Hedayati, B. H. Stark, and P. H. Mellor, "The impact of temperature and switching rate on dynamic transients of high-voltage silicon and 4H-SiC NPN BJTs: a technology evaluation," *IEEE Transactions on Industrial Electronics*, vol. 67, no. 6, pp. 4556-4566, 2020. https://doi.org/10.1109/TIE.2019.2922918.

[21] S. L. Kosier, A. Wei, R. D. Schrimpf, D. M. Fleetwood, M. D. DeLaus, R. L. Pease, et al., "Physically based comparison of hot-carrier-induced and ionizing-radiation-induced degradation in BJTs," *IEEE Transactions on Electron Devices*, vol. 42, no. 3, pp. 436-444, 1995. https://doi.org/10.1109/16.368041.

[22] S. S. Attar, "Development of an electrothermal simulation tool for integrated circuits," M. S. thesis, Ryerson University, 2023. https://doi.org/10.32920/ryerson.14657712.v1.

[23] L. Zhang, "High-performance SiC-based power semiconductor devices," Ph.D. dissertation, University of Warwick, Coventry, U.K., 2023. [Online]. Available: https://wrap.warwick.ac.uk/id/eprint/180281/. [Accessed Dec. 25, 2025].

[24] S. Baccar, T. Lévi, D. Dallet, V. Shitikov, and F. Barbara, "A behavioral and temperature measurements-based modeling of an operational amplifier using VHDL-AMS," In Proc. 17th IEEE International Conference on Electronics, Circuits and Systems, Athens, Greece, 12-15, Dec. 2010, pp. 343-346. https://doi.org/10.1109/ICECS.2010.5724523.

[25] G. V. Perov and M. A. Shevalye, "Effect of heat treatment on performance characteristics of operational amplifier," In Proc. International Conference and Seminar on Micro/Nanotechnologies and Electron Devices, Novosibirsk, Russia, 30 June-4 July, 2010, pp. 191-192. https://doi.org/10.1109/EDM.2010.5568832.

[26] Z. Yang, J. Li, J. Fu, J. Song, Q. Cai, S. Qiao, "A 250 °C low-power, low-temperature-drift offset chopper-stabilized operational amplifier with an SC notch filter for high-temperature applications," *Applied Sciences*, vol. 15, no. 2, p. 849, 2025. https://doi.org/10.3390/app15020849.

[27] V. S. Bendre and A. K. Kureshi, "Design and PVT analysis of robust, high swing folded cascode operational amplifier," *International Journal of Engineering and Advanced Technology*, vol. 9, no. 2, pp. 114-118, 2019. https://doi.org/10.35940/ijeat.b2995.129219.

[28] S. Baccar, T. Levi, D. Dallet, V. Shitikov, and F. Barbara, "A validity study of an industrial SPICE-based op-amp macromodel for high-temperature simulation," In Proc. IEEE International Instrumentation and Measurement Technology Conference, Graz, Austria, 13-16 May 2012, pp. 1294-1298. https://doi.org/10.1109/I2MTC.2012.6229463.

[29] S. C. Terry, B. J. Blalock, J. R. Jackson, Suheng Chen, M. M. Mojarradi, E. A. Kolawa, et al., "Development of robust analog electronics at the University of Tennessee for NASA/JPL extreme environment applications," in Proc. Biennial University/Government/Industry Microelectronics Symposium, Boise, ID, USA, 2 Jun. 2003, pp. 124-127. https://doi.org/10.1109/UGIM.2003.1225711.

[30] M. Lin, "Smart sensor for current leakage detection for EV charger station," [Online]. Available: http://202.28.34.124/dspace/handle/123456789/2681. [Accessed Dec. 25, 2025].

[31] Z. Wang, "A 45nm CMOS temperature sensing interface for crystal frequency temperature compensation," M.S. thesis, Carnegie Mellon University, Pittsburgh, PA, USA, 2009.

[32] K. Górecki, J. Zarębski, P. Górecki, and P. Ptak, "Electrothermal characteristics of the selected semiconductor devices," *International Journal of Electronics and Telecommunications*, vol. 65, no. 2, pp. 295-300, 2019. https://doi.org/10.24425/ijet.2019.126295.

[33] H. Zhu, "High efficiency base drive designs for power converters using silicon carbide bipolar junction transistors," Ph.D. dissertation, University of Sheffield, Sheffield, U.K., 2019.

[34] M. Nawaz, N. Chen, F. Chimento, and L. Wang, "Static and dynamic characterization of high power silicon carbide BJT modules," *IEEE Transactions on Industry Applications*, vol. 52, no. 6, pp. 4990-4998, 2016. https://doi.org/10.1109/TIA.2016.2600651.

[35] S. G. Sundaresan, A.-M. Soe, S. Jeliazkov, and R. Singh, "Characterization of the stability of current gain and avalanche-mode operation of 4H-SiC BJTs," *IEEE Transactions on Electron Devices*, vol. 59, no. 10, pp. 2795-2802, 2012. https://doi.org/10.1109/TED.2012.2210048.